

# GENERATION OF SPECTRAL AND TIMING PROPERTIES OF CYGNUS X-2 USING ASTROSAT'S DATA

Vanzarmawii Chhangte\*<sup>1</sup>, Ranjeev Misra<sup>2</sup>, Lalthakimi Zadeng<sup>1</sup>

<sup>1</sup>*Department of Physics, Mizoram University, Tanhril-796004, Aizawl, Mizoram, India*

<sup>2</sup>*Inter-University Centre for Astronomy and Astrophysics, Geneshkhind, Pune-411007, India*

\*For correspondence. (zarichhangte0739@gmail.com)

---

**Abstract:** We present here AstroSat LAXPC and SXT observation of an X-ray Binary source focusing on neutron stars. X-ray binaries are a class of binary stars, so-called because they emit X-ray. These X-rays are produced by matter falling from one component called donor to another component, accretor. The donors are usually normal stars and accretor are collapsed stars which are very compact e.g. neutron stars, white dwarf or black hole. We have taken into study, Cygnus X-2, which is a 9.84 day period neutron star binary belonging to long-period low-mass X-ray binary type. It is one of the brightest and longest known X-ray source. Three observations are studied for which lightcurves are generated with time bin of 100s each for LAXPC and 23s each for SXT. Hardness ratios are plotted from the generated lightcurve. Spectra and power spectra are also generated within the energy range 4.0-80.0 keV for LAXPC and 0.3-8.0keV for SXT. Further analysis of these spectral and timing properties will be done. For timing analysis, Fourier transform is used and spectra will be fitted using  $\chi^2$  fitting.

**Keywords:** accretion; accretion discs; stars: neutron; stars: individual: Cygnus X-2; X-rays: binaries

---

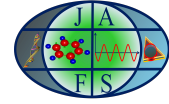
## 1. Introduction:

Binary stars are two stars orbiting around a common center of mass. The brighter is classified as the primary star and the dimmer is classified as secondary star. Matter is accreted from the companion by the compact object through Roche Lobe overflow or stellar wind accretion. The accreted matter from the companion flows onto the compact star through the influence of its gravitational potential. The inflowing matter has an accretion rate associated with it, so it spirals into the compact star forming an accretion disk. Because of the violent collisions between the particles in the inflowing matter the gas is heated to very high temperatures of about  $10^7$  K to  $10^8$  K. It is through this process that the gravitational potential energy of the infalling matter gets converted to the kinetic energy and then into radiation in the form of X-rays.

X-ray Binaries(XRB) are of two types depending on the mass of the mass losing star (companion star): Low-mass XRB (LMXB) and High-mass XRB (HMXB). In LMXB the donor star have a mass of about  $1M_{\odot}$ . LMXB fill their Roche lobe and transfer of mass takes place by accretion of matter through inner Lagrangian point. The neutron star here has weak magnetic field of about  $10^7$  to  $10^9$  Gauss, therefore the accreted matter does not fall onto the magnetic poles. They have a very pronounced accretion disk and a vast majority of the produced X-rays are from the inner part of the disk and the surface of the neutron star. X-rays are also found to be produced from the accretion disk corona which is the extended region above and below the disk. The wind material driven off of the disk produces extended corona. X-rays are scattered by hot plasma in the disk from the corona.

In HMXB, the donor star have mass  $\leq 10M_{\odot}$ . Most of its mass is lost due to powerful stellar wind of the companion star. Mass transfer in HMXB systems takes place by powerful accretion of some part of the matter from the stellar wind of the companion star by the compact object. They do not have distinct accretion disk and the accretor in HMXBs may be a neutron star or a black hole. Here the neutron stars have high magnetic field of about  $10^{12}$  Gauss.

The source, Cygnus X-2 is a LMXB, consisting of a neutron star with an optically measured mass of  $M_x > 1.78 \pm 0.23M_{\odot}$  [3] orbiting around V1341 Cyg with an orbital period of  $\sim 9.8$  days [1, 2]. Cyg X-2 is a bright



and persistent source and is classified as a Z source because of its behaviour when studied on an X-ray color-color diagram (CCD). They follow a 1-D path in 2- dimensional CCD, and as the source moves between different spectral states, they trace out a Z shape. The top part of the Z shape is referred to as the horizontal branch (HB), the diagonal part is called the normal branch (NB) and the base of the Z shape is referred to as the flaring branch (FB).

Cygnus X-2, like other Z sources have complex X-ray spectrum leading to the need of superposition of several spectral components.

The observatory used here is ASTROSAT (Astro Satellite) and is India's first multi-wavelength space observatory. It observes in the optical (400-700nm), UV (10-310nm), low and high energy X-ray (0.01-10nm) regions of the electromagnetic spectrum. It carries 5 payloads: The Ultraviolet Imaging Telescope (UVIT), Large Area X-ray Proportional Counter (LAXPC), Soft X-ray Telescope (SXT), Cadmium Zinc Telluride Imager (CZTI) and Scanning Sky Monitor (SSM).

Generation of the spectral and timing properties of Cyg X-2 is done here while interpretation will be done as the work progresses further.

## 2. Data reduction:

The source, Cygnus X-2 was observed by AstroSat's LAXPC and SXT, three observations were taken during the time period from June 2018-July 2019. We have downloaded data from Astrobrowse. We analyse the data for both LAXPC and SXT using their respective softwares, LAXPCSoft and SXT Software.

For LAXPC:

We set the variable path to where our data is in the directory where we want to keep the results of the analysis. With LAXPCSoft command we make data file lists, create FITS event file and the gti file which has the Good Time Intervals (GTI), this removes earth's occultation and SAA. After these preliminary steps we can create the lightcurves, spectra, power spectra and time lags with defined flags.

We use the "laxpc\_make\_lightcurve" command to generate the lightcurve with suitable flags.

For SXT:

SXT data are converted into FITS files at the Indian Space Science Data Center (ISSDC). From ISSDC website the Level2 Pipeline Software and Calibration Database can be downloaded.

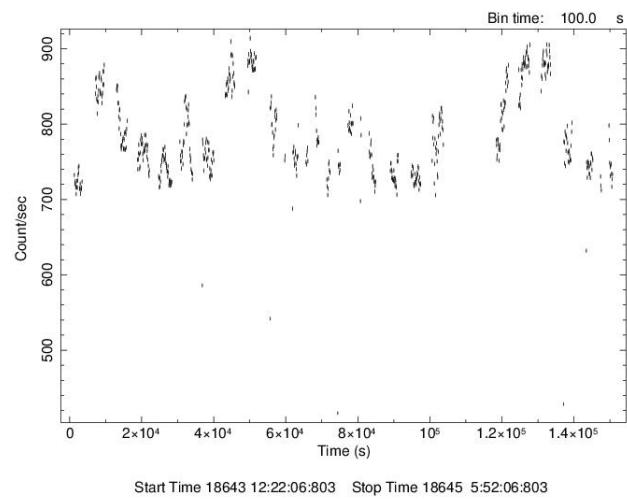
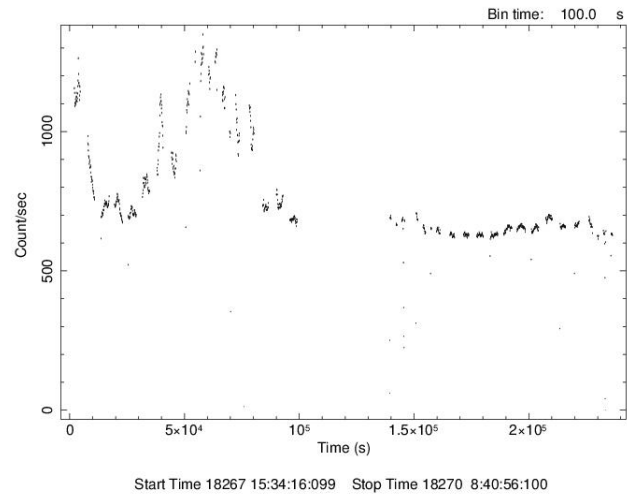
There are three stages of the pipeline that include standard calibration, screening, where level2 events data are screened with 'xselect' tool to produce GTIs and higher order product generation that can be read into multi-mission data analysis programs such as XSPEC, XRONOS and XIMAGE respectively.

For all the three stages of analysis 'sxtpipeline' is the usual starting point in the reduction of ASTROSAT's SXT data. It uses level1 files, parameter files and calibration database available at the time of processing.

We merge the level2 clean event files using julia software and xselect tool was used to extract the image of the cleaned event file. We got the lightcurve and the spectra by selecting an annular ring of radius 12 and 6 arcmin respectively around the source. We then extract the lightcurve and spectra.

(a) Lightcurve:

LAXPC covers an energy range of 4.0-80.0keV. In this case we have taken the timebin to be of 100s each and energy was taken for 4.0-10.0 keV. We have set p to be 2 (LAXPC 20). We have cleaned the lightcurves and the generated lightcurves for the three observation IDs- 9000002130, 9000002982 and 9000003064, are given below.



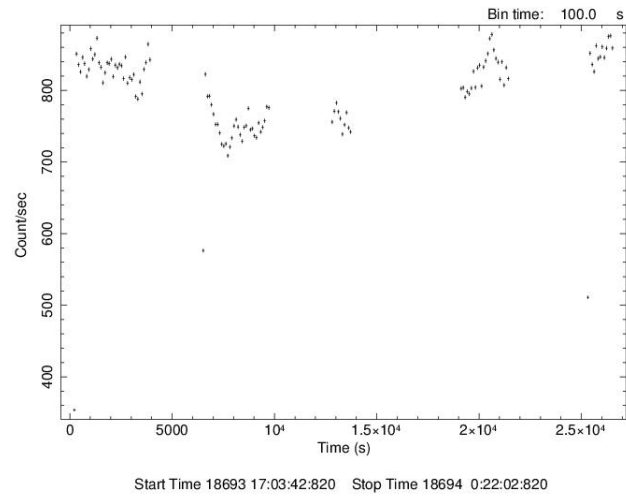
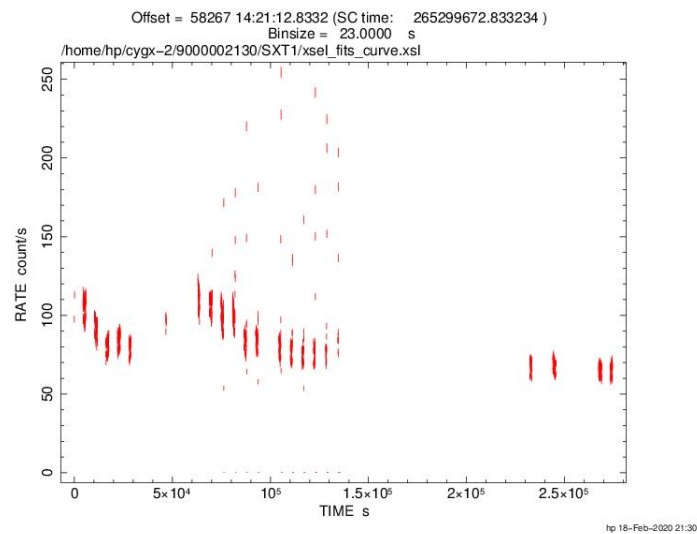


Figure 1: Top: Obs ID 9000002130; Middle: Obs ID 9000002982; Bottom: Obs ID 9000003064. LAXPC lightcurves with energy range 4.0-80.0keV.

For SXT, lightcurves were generated with a time bin of 23s for each observation. SXT covers an energy range of 3.0-8.0keV.



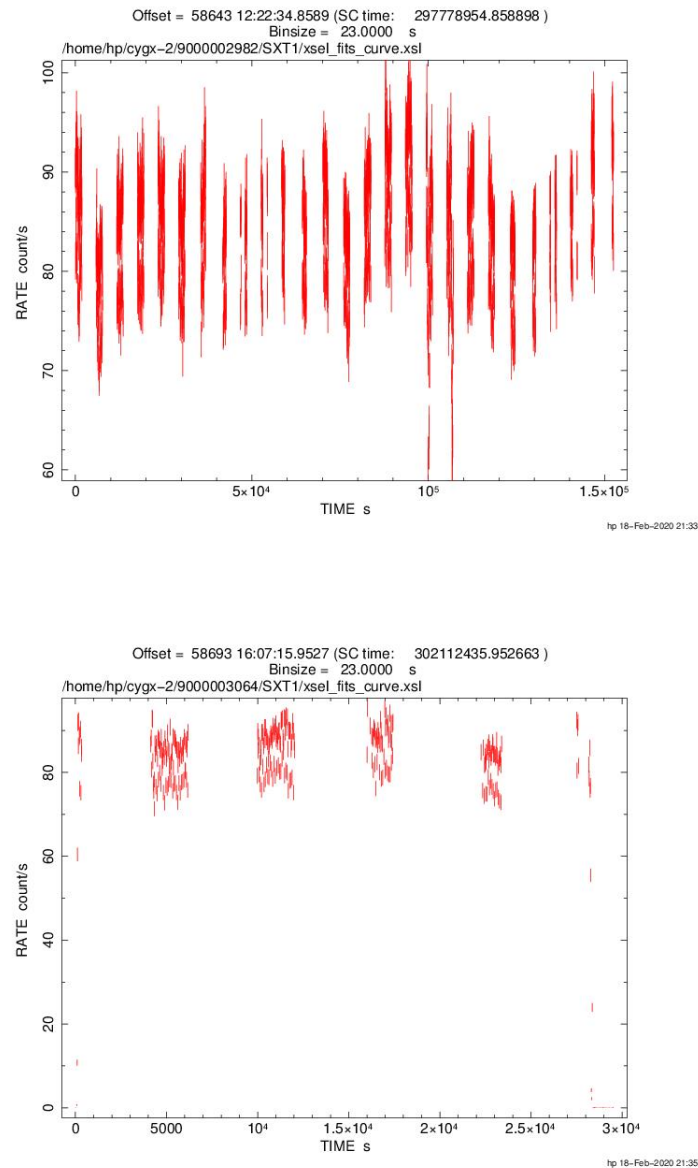


Figure 2: top: Obs ID 9000002130; Middle: Obs ID 9000002982; Bottom: Obs ID 9000003064. SXT lightcurves with energy range 3.0-8.0keV.

(b) Hardness intensity ratio

From the extracted lightcurves in 4.0-8.0keV and 8.0-10.0keV bands with 100s timebins for all three observations, we got the combined hardness intensity diagram which is the ratio of count rate in the energy band 4.0-8.0keV and 8.0-10.0keV.

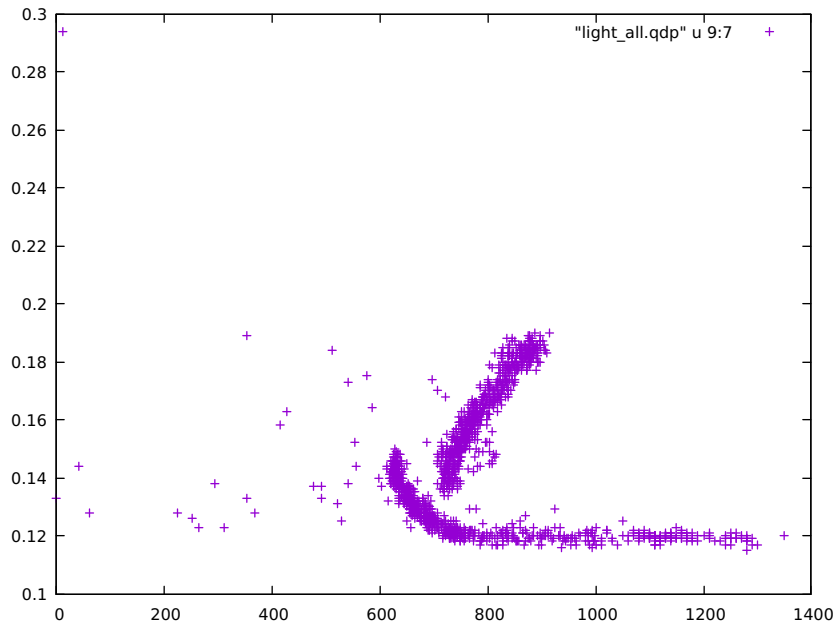


Figure 3: Hardness intensity diagram.

### (c) Spectral timing

For LAXPC, we extract the spectra with “laxpc\_make\_spectra” comand and the background spectra is generated using the LAXPCSoft command “laxpc\_make\_backspectra” with defined flags for both cases.

For SXT, we extract the spectra using xselect after image and lightcurve have been generated for energy band 0.3-8.0keV.

$\chi^2$  fitting is used for determining the best-fit model, defined as:

$$\chi^2 = \sum \frac{(C(I) - C_P(I))^2}{(\sigma(I))^2}$$

where  $C(I)$  is the observed data,  $C_p(I)$  is the predicted count spectrum,  $\sigma(I)$  is the (generally unknown) error for channel  $I$  (e.g., if  $C(I)$  are counts then  $\sigma(I)$  is usually estimated by  $\sqrt{C(I)}$ ).

The “goodness-of-fit” of the model:

The  $\chi^2$  statistic provides a well-known-goodness-of-fit criterion for a given number of degrees of freedom ( $\nu$ , which is calculated as the number of channels minus the number of model parameters) and for a given confidence level. If  $\chi^2$  exceeds a critical value (tabulated in many statistics texts) one can conclude that  $f_b(E)$ (model spectrum) is not an adequate model for  $C(I)$ . As a general rule, one wants the “reduced  $\chi^2$ ” ( $\sim \chi^2/\nu$ ) to be approximately equal to one (i.e.  $\chi^2 \sim \nu$ ). A reduced  $\chi^2$  that is much greater than one indicates a poor fit, while a reduced  $\chi^2$  that is much less than one indicates that the errors on the data have been over-estimated. Even if the best-fit model ( $f_b(E)$ ) does pass the “goodness-of-fit” test, one still cannot say that  $f_b(E)$  is the only acceptable model. For example, if the data used in the fit are not particularly good, one may be able to find many different models for which adequate fits can be found. In such a case, the choice of the correct model to fit is a matter of scientific judgment.

Fitting is done using xspec version 12.10.1f. To begin with, we first combine the spectra of both LAXPC and SXT. The red lines indicate the spectra for SXT while the black lines are for LAXPC.

We fitted the X-ray continuum of Cyg X-2 with a blackbody or disk multicolor blackbody (diskbb), with tbabs,compTT and power law. The best fit to the continuum of Cyg X-2 was obtained using a blackbody or a diskbb. The normalisation of diskbb can be calculated using

$$K = (R_{in}/D_{10})^2 \cos\theta$$

where  $D_{10} = d/10$ ,  $d=7.2\text{kpc}$  and  $\theta = 62^\circ.5$

For bbody, normalisation is calculated using

$$K = L_{39}/D_{10}^2.$$

The luminosity of Cyg X-2, taken here was  $\leq 2 \times 10^{36}\text{ergs s}^{-1}$  [4]

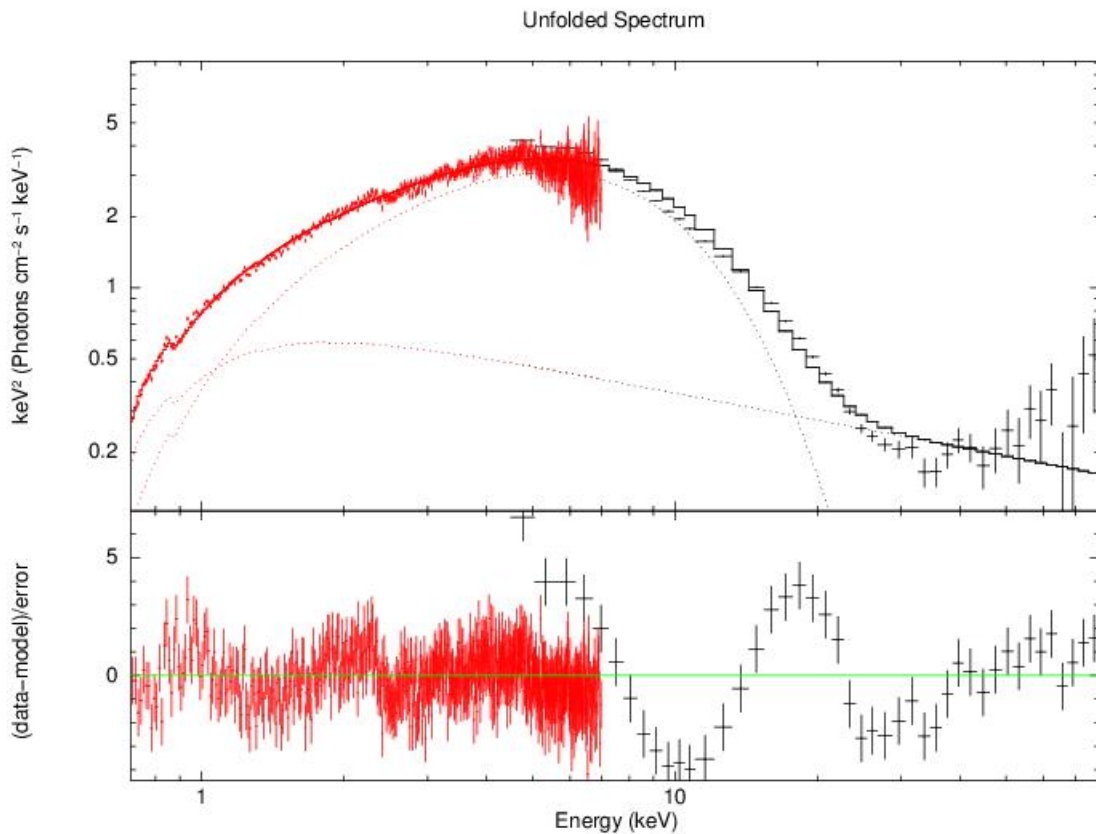


Figure 4: Spectra of Cyg X-2 fitted with tbabs\*(diskbb+pow).

Table 1: Table for error for model tbabs, diskbb and powerlaw.

Model Parameter	Confidence Range
nH	0.280702, 0.306478 (-0.0129984, 0.0127782)
$kT_{in}$	2.25231, 2.28435 (-0.0159279, 0.161168)
$N_{disk}$	16.9648, 18.0127 (-0.516556, 0.531287)
$\Gamma$	2.35717, 2.40951 (-0.0265988, 0.0257357)
K(powerlaw)	0.806042, 0.927511 (-0.0604658, 0.0610033)

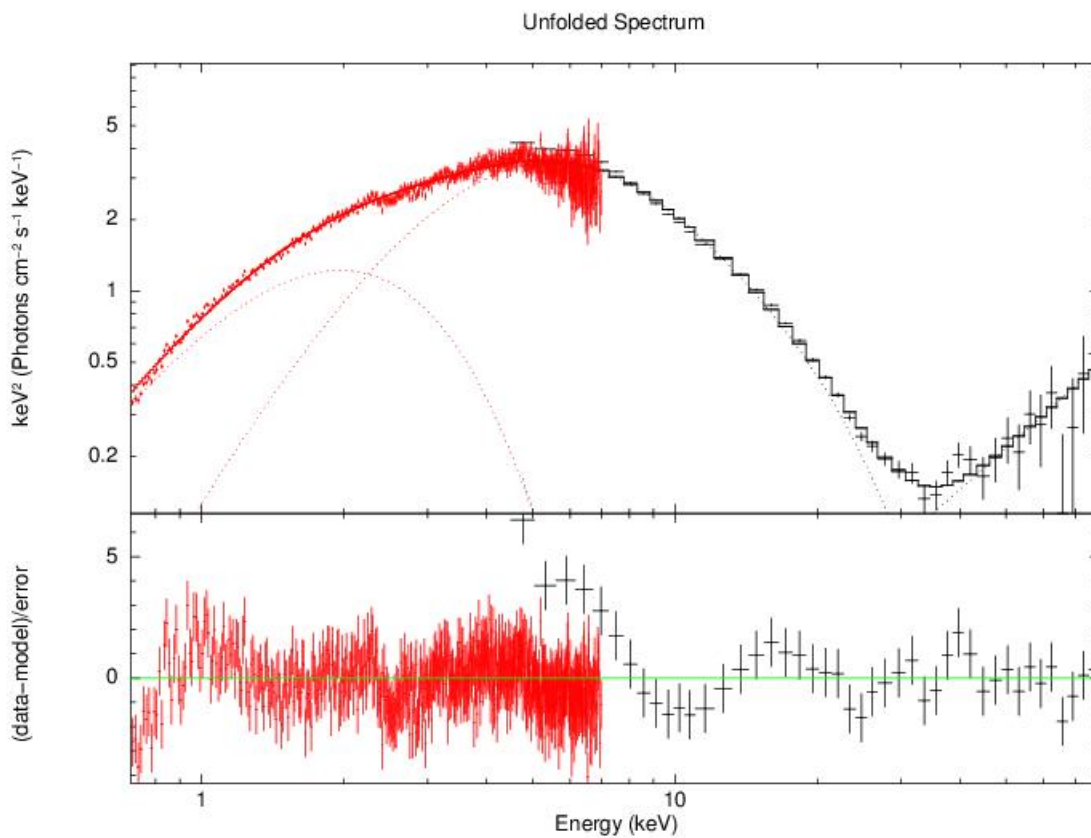


Figure 5: Spectra of Cyg X-2 fitted with bbody+compTT+pow.

Table 2: Table for error for model bbody, compTT and powerlaw.

Model Parameter	Confidence Range
$K_{bb}$	0.0313365, 0.03206 (-0.000365123, 0.000358397)
$T_0$	1.16028, 1.19481 (-0.0177065, 0.0168255)
$kT_e$	3.5263, 4.26704 (-0.0330748, 0.409989)
$\tau_p$	2.59908, 3.29483 (-0.35404, 0.341708)
$N_{compTT}$	0.37962, 0.476705 (-0.0489708, 0.0481137)
$\Gamma$	-0.2881438, 0.797153 (-0.52362, 0.554971)
K(powerlaw)	2.3657e-05, 0.00151853 (-0.000200407, 0.00129446)



3. Results and discussion:

From the generated lightcurves of LAXPC and SXT in figures 1 and 2, we see that it is in par with what is expected from a LMXB. X-ray dips could be seen from the lightcurves. We can see how the LAXPC and SXT lightcurves correspond with each other. The brightness varies with each observation depending on the time at which it is taken.

Fig.3 is the Hardness Intensity Diagram for the combined observation of Cyg X-2. It is seen that HB is not visible in the HID and the source seem to move along the HB and FB of its Z-track.

Fig.4 is the spectra fitted with tbabs, diskbb and powerlaw. The parameters of the diskbb component varies significantly with position along the Z track, with varying inner disk temperature  $kT_{in}$  and the inner radius  $r_{in}$  changing from 34 to 25 km [4]. We have found the  $\chi^2$  value to be 1.4.

Fig.5 is fitted with bbody, compTT and powerlaw. The bbody temperature was taken at  $kT_{bb} \sim 0.5\text{keV}$  and the calculated normalisation value  $\sim 3.4 \times 10^{-2}$  was used. The  $\chi^2$  value obtained was 1.3.

Tables 3 and 4 summarises some of the relevant parameters for both the models used.

Table 3: Spectral fit parameters for models: tbabsx(diskbb+powerlaw).

Model Parameters	Values
$kT_{in}(\text{keV})$	$2.26^{+9.5E-03}_{-9.5E-03}$
$N_{disk}$	$17.48^{+0.31}_{-0.31}$
$\Gamma$	$2.38^{+1.6E-02}_{-1.6E-02}$
Reduced $\chi^2=1.4$	

Table 4: Spectral fit parameters for models: bbody+compTT+powerlaw.

Model Parameters	Values
$kT_{bb}(\text{keV})$	$0.5^f$
$K_{bb}$	$3.4E-02^{+2.28E-04}_{-2.28E-04}$
$kT_e(\text{keV})$	$3.7^{+0.25}_{-0.25}$
$\Gamma$	$0.24^{+0.40}_{-0.40}$
Reduced $\chi^2=1.3$	

Here we have covered the generation of spectral and timing properties of a LMXB Cygnus X-2, interpretation will be done as the research progresses further.

References:

[1]Casares J., Charles P., Kuulkers E. (1998). The Mass of the Neutron Star in Cygnus X-2(V1341 Cygni). *The ApJ*, **493**, 39-42.  
 [2]Cowley A. P., Crampton D., Hutchings,J. B. (1979). The halo population X-ray Source Cygnus X-2, *The ApJ*, **231**, 539-550.  
 [3]Orosz J. A and Kuulkers E. (1999). The optical light curves of Cygnus X-2 (V1341 Cyg) and the mass of its neutron star, *MNRAS*,**305(1)**, 132-142.  
 [4]Piraino S., Santangelo A., Kaaret P. (2001). X-ray Spectral and Timing Observations of Cygnus X-2, *The ApJ*, **567**, 1091-1101.  
 [5]Ramdevi M. C. X-ray Binaries.